Growth Mechanism of Hexagonal-Shape Graphene Flakes with Zigzag Edges

Zhengtang Luo,[†] Seungchul Kim,[‡] Nicole Kawamoto,[†] Andrew M. Rappe,[‡] and A. T. Charlie Johnson[†,*]

[†]Department of Physics and Astronomy, University of Pennsylvania, Philadelphia, Pennsylvania 19104-6396, United States and
[‡]The Makineni Theoretical Laboratories, Department of Chemistry, University of Pennsylvania, Philadelphia, Pennsylvania 19104-6323, United States

ABSTRACT

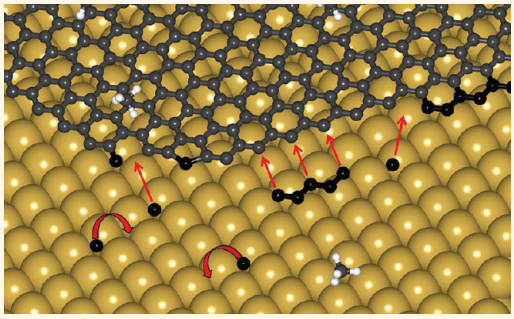

The properties of a graphene nanostructure are strongly influenced by the arrangement of the atoms on its edge. Growing graphene nanostructures with specified edge types in practical, scalable ways has proven challenging, with limited success to date. Here we report a method for producing graphene flakes with hexagonal shape over large areas, by a brief chemical vapor deposition growth at atmospheric pressure on polished Cu catalyst foil, with limited carbon feedstock. Raman spectra show evidence that the edges of the hexagonal crystallites are predominantly oriented along the zigzag direction. Density functional theory calculations demonstrate that the edge selectivity derives from favorable kinetics of sequential incorporation of carbon atoms to the vacancies in nonzigzag portions of the edges, driving the edges to pure zigzag geometry. This work represents an important step toward realization of graphene electronics with controlled edge geometries, which might find use in digital logic applications or zigzag-edge-based spintronic devices.

KEYWORDS: graphene · chemical vapor deposition · zigzag edges · density functional theory · growth mechanism · carbon adatom

Edge atoms and their arrangement can control the properties of 2D nanometer-scale materials, similar to the surface atoms of 3D nanostructures.[1,2] For example, it was predicted that engineering the edge structure of a graphene nanoflake can open an energy gap in graphene nanoribbons (GNR)[3] that is exquisitely sensitive to atomic disorder[4,5] and that a unique spin state exists at the edges of zigzag GNRs with half-metallic behavior under an applied electric field.[6] Although crystallographically oriented edge structures were occasionally observed (by micromechanically exfoliating graphene flakes,[7,8] by etching holes with oxidants,[9] by irradiating with an electron beam,[10] and by etching trenches in multilayer graphene flakes with nanoparticles[11]), experimental success in controlled synthesis of graphene flakes with accurate edge atom arrangement has been limited. Having graphene flakes with defined edge configurations would provide a path toward greater insight into the role of edges in the transition from 2D extended monolayer properties to 1D nanoribbon behavior, which is of practical and fundamental importance. Here we report the formation of graphene structures dominated by zigzag edge structures. Experimental characterization and computer modeling are combined to reveal the mechanism of zigzag edge selectivity and the formation of highly crystalline graphene.

RESULTS AND DISCUSSION

Chemical vapor deposition (CVD) of graphene on polycrystalline Cu foil is a low-cost approach to the synthesis of large-area graphene.[12,13] Others have reported the growth of regular hexagonal graphene crystallites with edges mostly aligned along the zigzag direction, although this observation was complicated by damage to the hexagons incurred during transfer to the electron microscopy support.[14] We recently developed[15] an atmospheric pressure CVD method to grow high-quality graphene, which involves the use of an electropolished, very smooth Cu catalyst surface and a very low concentration of carbon in the feedstock gas. To investigate this growth method further, we quenched the reaction before a full graphene monolayer is grown on the Cu catalyst. Figure 1a provides scanning electron microscopy (SEM) images of graphene flakes produced in a 5 min growth

* Address correspondence to cjohnson@physics.upenn.edu.

Received for review September 1, 2011 and accepted October 14, 2011.

Published online October 15, 2011
10.1021/nn203381k

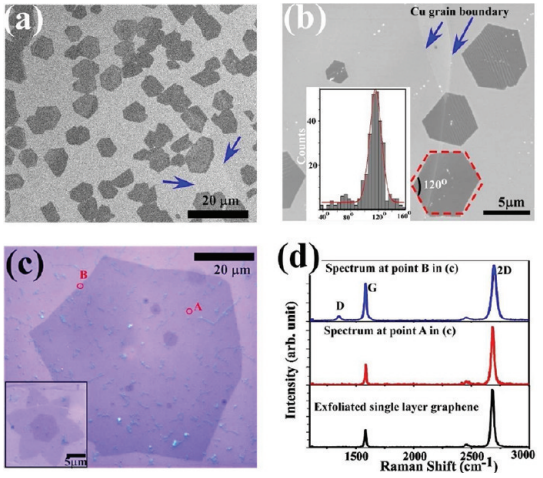

Figure 1. Graphene flakes with hexagonal shapes. (a) SEM images of graphene flakes on Cu foil. Arrows indicate Cu grain boundaries. (b) Higher magnification SEM images show that the graphene flakes retain their hexagonal shape when crossing grain boundaries. Inset shows the statistics of angles between two edges. (c) Graphene flakes with ~70 μm diameter. Inset shows a hexagram shape stacked with a hexagonal flake. (d) Raman spectra taken at locations A and B in panel (c), compared to that from a single-layer graphene flake obtained by mechanical exfoliation.

using 41 ppm of methane as carbon feedstock. The graphene crystallites are predominantly hexagonal in shape, with 120° angles between adjacent edges (see histogram in inset of Figure 1b). The graphene hexagons are apparently only weakly coupled to the Cu surface, as they are frequently observed to have grown across Cu grain boundaries and on rougher regions of the surface (Figure 1b). Flakes as large as ~75 μm in diameter (Figure 1c) may be grown simply by controlling the growth time. Other 6-fold symmetric structures were also observed, as shown in the inset of Figure 1c, where a stack of a hexagram and hexagon is seen.

This hexagonal shape is very different from the curved shapes reported to grow on other close-packed single-crystal surfaces of metals, such as Ru(001)[16,17] and Ir(111).[18] For example, graphene seeds grown on Ru(001) show strong coupling to the substrate, resulting in graphene flakes with unsymmetrical shapes. Hybridization of the out-of-plane graphene π orbitals with metal *d* bands is apparently strong enough to disrupt graphene growth when it reaches a step edge.[16] In addition, the hexagonal graphene shapes in Figure 1 are strikingly different from crystallite shapes observed after Cu-catalyzed CVD growth under high vacuum, even though the process was otherwise similar to that used here. High-vacuum CVD growth is reported to result in graphene crystallites that grow into four-lobed ("flower-like") structures, until interrupted by other graphene seeds or by Cu surface imperfections.[12,19,20] Theoretical and experimental investigations show that the flower-like structure arises from growth that is dominated by edge kinetics with

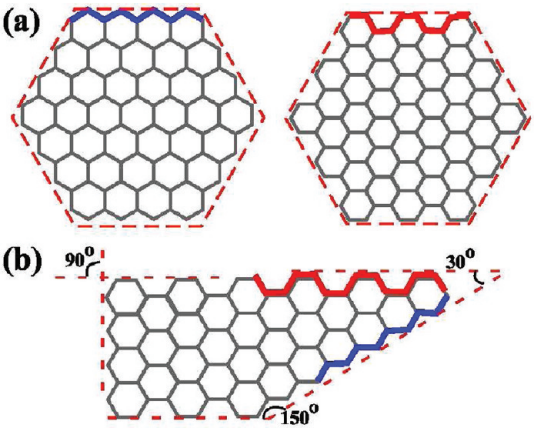

Figure 2. Schematic view of angles formed between two graphene edges. Graphene flakes with solely armchair or solely zigzag edges are hexagonal in shape, while angles formed where a zigzag edge meets an armchair edge are $(2n - 1) \times 30°$ (n = 1, 2, ...).

an angularly dependent growth velocity, where the fast growth direction is not aligned with a high-symmetry axis of graphene. Each lobe generally has a different crystallographic orientation, so these graphene flower-like flakes are not single crystals.[20]

Figure 2 illustrates the possible angles between graphene edges that are aligned with the zigzag or armchair directions. For graphene flakes with only pure zigzag or armchair edges (left and right images in Figure 2a, respectively), the angles formed between the edges are $2n \times 30°$ (n = 1, 2, 3, ...). In contrast, graphene flakes with neighboring zigzag and armchair edges will have angles of $(2n - 1) \times 30°$ (*e.g.*, 30°, 90°, 150°). This simple analysis leads to a straightforward but useful conclusion: flakes with 6-fold symmetric shapes, such as hexagon and hexagram, could be bounded by only zigzag or only armchair edges. As described below, we have experimental evidence from Raman spectroscopy that the edges of the hexagonal crystallites produced in this work are predominantly zigzag in their orientation, in agreement with our computational investigations on stabilities of intermediate structures of edge growth.

The Raman spectrum shown in the middle panel of Figure 1d was taken at location A of Figure 1c and is typical of a large number of spectra taken at positions away from the edges of the graphene flakes. These spectra are essentially identical to the Raman spectrum "fingerprint" characteristic of single-layer graphene samples produced by the standard micromechanical exfoliation process (bottom panel of Figure 1d). This indicates that the hexagonal flakes are single layers;[15] in combination with the preceding geometrical analysis, this finding suggests that their edges are likely dominated by either zigzag or armchair structures. In addition, the ratio of the D to G peak intensity I(D)/I(G) may be used to identify zigzag edges,[9,21] which give very low I(D)/I(G) values near 0.05 for graphene flakes

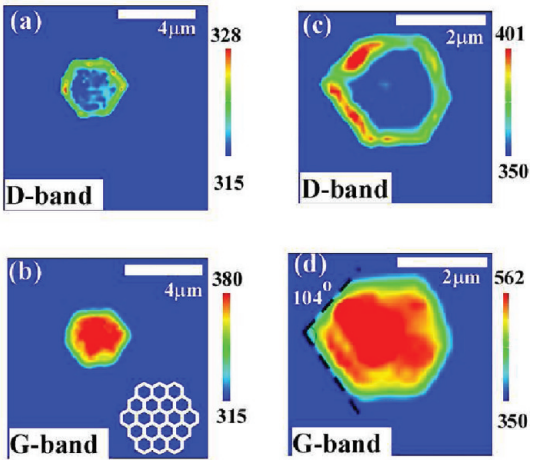

Figure 3. Raman map of hexagonal flakes of CVD-grown graphene collected using a laser excitation wavelength of 532 nm. (a and b) D and G band intensity map for a flake with six corner angles all close to 120°. (c and d) D and G band intensity map for a flake with one corner angle that differs significantly from 120°.

obtained by micromechanical exfoliation, in contrast to intensity ratios near 0.3 reported for rounded edges or armchair edges.[8] The *I*(D)/*I*(G) values obtained from single spectra taken at the edges of hexagonal graphene flakes, as well as those obtained from Raman mapping as described in the next paragraph, are typically less than 0.1, as shown in the top panel of Figure 1d. The fact that we observe a slightly higher *I*(D)/*I*(G) ratio than the earlier reports presumably reflects the presence of more defects in our samples, compared to exfoliated flakes, due to a combination of the intrinsic properties of CVD graphene and the acid treatment used in the transfer from the Cu growth substrate. This provides strong evidence that the edges of the hexagonal graphene flakes are predominantly zigzag.

Raman mapping with an illumination wavelength of 532 nm was also performed to gain structural information regarding the graphene edges. Figure 3 shows spatial maps of the D- and G-band Raman intensities for a flake with nearly perfect hexagonal structure, as well as a flake with one corner whose angle significantly differs from 120°. In both flakes, the D-band intensity is predominantly localized at the edge, while the G-band intensity increases from the edge to the center, as more carbon atoms are illuminated by the laser. For the flake with all six angles close to 120° (Figure 3a,b), no significant D-band intensity variation is observed on the six edges, indicating the homogeneity of the edge structure. After subtraction of the Raman background, the observed values of the *I*(D)/*I*(G) ratio at the edges are in the range 0.05−0.1, consistent with the Raman spectra of Figure 2d, taken at a slightly different laser wavelength of 514 nm. In contrast, for the irregularly shaped graphene flake (Figure 3c,d), the two edges that define the angle that significantly differs from 120° have significantly larger D-band intensity than the four other edges, with an *I*(D)/*I*(G) ratio of approximately 0.25. The Raman data alone do not allow us to assign the edge geometry conclusively, but it is highly likely these two edges are neither pure zigzag nor armchair. Our assignment of the zigzag edge geometry for graphene flakes with regular hexagonal geometry is consistent with electron diffraction data obtained by others from graphene crystallites derived using a similar growth process.[14]

Density functional theory (DFT) calculations were performed to determine the geometries and energetics of various graphene nanoflakes, to understand relationships between fragment shape, edge type, and interaction with a copper slab. Our DFT calculations are performed with a plane-wave basis set[22] and pseudopotentials,[23,24] using the generalized gradient approximation (GGA-PBE).[25] Details of the methods are presented in the Supporting Information. We examined the energetics of straight edges and then studied the stability of adatoms attached at straight edges or at boundaries between adjacent zigzag and armchair edges.

The total energy of an adsorbed graphene flake relative to an isolated extended graphene sheet and a bare Cu substrate can be expressed as

$$\begin{aligned} E_{tot} &= \varepsilon_{vdW} S + \varepsilon_{edge} L \\ &= \varepsilon_{vdW} S + (\varepsilon^{P}_{edge} - \varepsilon_{G-Cu}) L \end{aligned} \quad (1)$$

Here, ε_{vdW} is the van der Waals interaction energy[26] per unit area, ε^{P}_{edge} is the edge formation energy of pristine graphene, and ε_{G-Cu} is the average bonding energy of the graphene edge to the Cu substrate per edge unit length. *L* and *S* are, respectively, the length of the edge and the surface area of the graphene flake. Because ε_{vdW} has no dependence on edge type, we ignored this term in our analysis. We calculated the edge formation energy (ε^{P}_{edge}) of pristine graphene by determining the energy difference between graphene nanoribbons (GNR and E_{GNR})[3] and graphene (G, E_G), per GNR edge length:

$$\varepsilon^{P}_{edge} = (E_{GNR} - E_G)/L \quad (2)$$

Figure 4a, along with Figure S1 in the Supporting Information, illustrates the atomic models we used to calculate the energies of graphene edges on a Cu slab. We chose the (100) face of Cu since our Cu foil surface was predominantly (100).[27] We examined two relative angles, $\theta_{G/Cu}$ = 0° and 45°, between the graphene edges and the square lattice of Cu(100), as well as several geometries for each of these angles. We calculated that the edge formation energy ε^{P}_{edge} and binding energy ε_{G-Cu} for the armchair (zigzag) edge were 1.00(1.13) and 0.65(0.74) eV/Å, respectively. Consequently, the net ε_{edge} values for armchair (zigzag) are

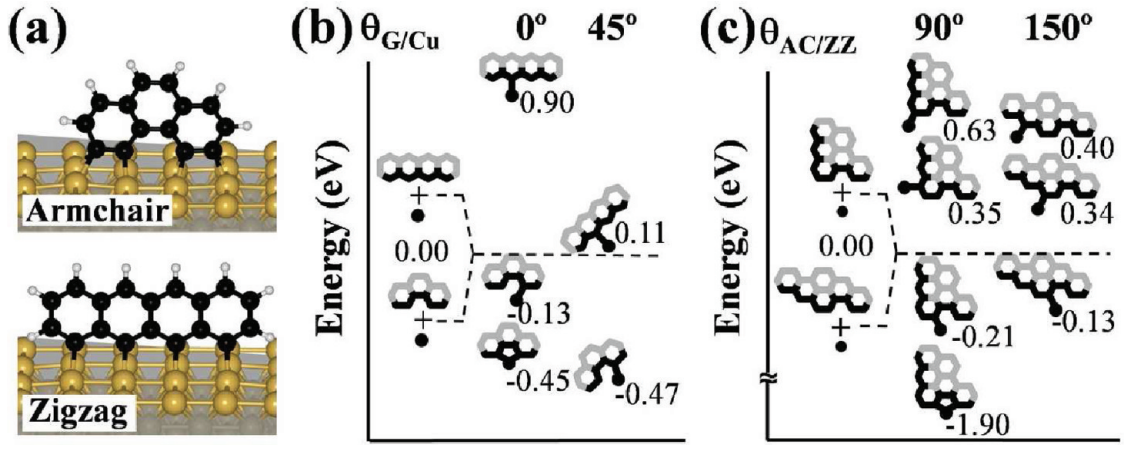

Figure 4. DFT-calculated stability of single carbon atom attachment at graphene edges in contact with Cu(100) surface. (a) Armchair and zigzag edges for a nanoflake oriented with an edge parallel to a Cu nearest-neighbor chain (denoted as $\theta_{G/Cu} = 0°$, where $\theta_{G/Cu}$ is the angle between the edge and the Cu chain). (b) Energies of a carbon adatom attached at zigzag and armchair straight edges with reference to separately adsorbed atom and edges (*i.e.*, 0 eV). Results are presented for $\theta_{G/Cu} = 0°$ and 45°. (c) The energies of adatom attachment to boundaries between adjacent armchair and zigzag edges with angles ($\theta_{AC/ZZ}$) of 90° and 150°. Gray, black, and black dots represent nonedge atoms, edge atoms, and adatoms, respectively. Results indicate that monatomic attachment to the zigzag edge or AC/ZZ boundary is energetically unstable, but single atoms bind to the armchair edge.

1.00−0.65 = 0.35 eV/Å = 0.86 eV per edge atom (1.13−0.74 = 0.39 eV/Å = 0.83 eV per edge atom). In agreement with previous reports,[28] these energies indicate that the zigzag and armchair edges have almost the same net formation energy on Cu, and, thus, neither edge is significantly favored. Additionally, the positive values of ε_{edge} show that the longer edges have higher net energy, and thus straight edges are preferred over curved ones.

In practice, graphene flake growth is more likely to be a nonequilibrium process, such that the kinetic conditions or the intermediate states may well play a vital role in graphene growth, perhaps even more important than the energetics of perfect edges. The key feature of the experimental method was to lower the carbon flux. Since the densities of clusters and monomers depend on the concentration of carbon precursors, we hypothesize that there is a growth mechanism in which the cluster density plays a critical role, namely, the shapes of graphene are different depending on whether they grow predominantly by cluster attachment or by monomer attachment. To test this hypothesis, first-principles calculations of the stability of adatoms attached at various edge geometries are performed. The energy (E) of an adatom attached at the edge is calculated as follows:

$$E = E_{G+1/Cu} - E_{G/Cu} - E_C^{atom} - E_C^{ads} \qquad (3)$$

E is the energy relative to separately adsorbed C atoms and graphene fragments. $E_{G+1/Cu}$ and $E_{G/Cu}$ are the total energies of adsorbed graphene fragments with and without an adatom, respectively. E_C^{atom} is the energy of an isolated carbon atom, while E_C^{ads} is the adsorption energy of a carbon atom on a Cu(100) surface, 6.10 eV. Figure 4b and c illustrate the calculated energies for the straight, zigzag, and armchair edges and boundary sites between them.

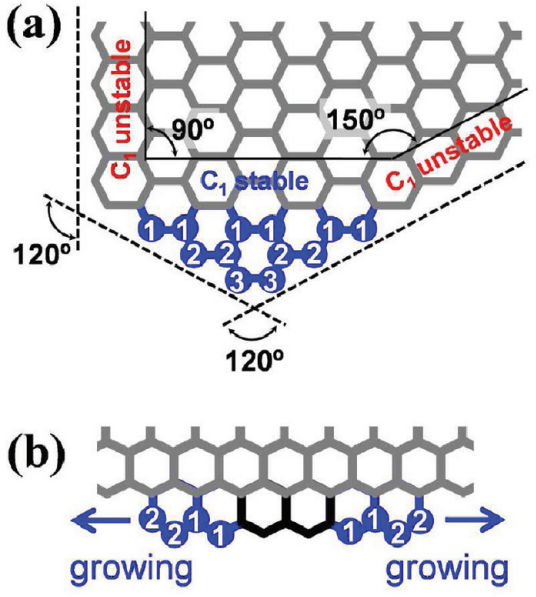

Figure 5. Edge-converting and zigzag edge growth mechanisms. (a) Schematic drawing of the mechanism by which nonzigzag edge is converted to zigzag. Gray lines indicate pre-existing graphene flake, sites labeled 1 are the stable sites where monomers can bind to the flake, and sites 2 (3) are sites where monomers can bind once the sites 1 (2) are occupied. Each new atomic row completes one fewer hexagon than the previous one, until the armchair edge disappears. 90° and 150° angles between edges are converted to 120° by monomer attachment at stable sites. (b) The growth mechanism of zigzag edges by monomer attachment is preceded by cluster attachment. Gray is a zigzag edge, black is an attached cluster, sites 1 are stable monomer sites, and sites 2 are stable monomer sites when sites 1 are occupied.

We draw attention to two findings: (1) monomers (single carbon adatoms) at zigzag edges are energetically unstable, while those at the armchair edges are stable, regardless of $\theta_{G/Cu}$; and (2) monomers at the armchair/zigzag (AC/ZZ) boundaries are unstable regardless of $\theta_{AC/ZZ}$, the angle between the two edges. The fact that monomers are unstable at any edge is surprising, because the C−C bond is much stronger than the C−Cu bond. For example, the formation energy of graphene from our calculation was 5.16 eV/bond, while the adsorption energy of a carbon monomer on Cu(100) was about 1.22 eV/bond (monomers are adsorbed at the 5-fold hollow site on the Cu surface, with 6.10 eV of adsorption energy).

Here, we assert a seemingly paradoxical attribute of monomer attachment to edges: *monomer attachment at an armchair edge shortens the armchair edge but lengthens the zigzag edges*. This phenomenon takes place when the aforementioned stabilities of monomers meet the honeycomb lattice of graphene. Monomers can grow armchair edges. However, the attachment of monomers shortens the edge, since the monomers are stable only inside the armchair edge (*e.g.*, sites 1 in Figure 5a), and thus new edge boundaries move inward to the armchair edge. Each new atomic row completes one fewer hexagon than the previous one, until the armchair edge disappears. This process is illustrated in Figure 5a. In this way, any nonzigzag edge segments, which must have an armchair segment, at least in part, will be filled out and converted to zigzag edge by monomer attachment.

Because monomers are unstable at the zigzag edges, cluster attachment is a key step for the growth of zigzag-edged graphene, but it need not be the dominant process of the growth. If a cluster attaches at the straight zigzag edge, stable binding sites for monomers are provided adjacent to the cluster. Figure 5b illustrates consecutive addition of atoms to the zigzag edge. After a cluster (black) attaches to the zigzag edge (gray), stable sites for monomer attachment (sites 1) are provided, and then additional stable sites (sites 2) become available after sites 1 are occupied. Monomers continue to attach adjacent to the growing cluster, until a whole zigzag chain is added to the pre-existing edge. We observed from the calculations using a six-unit cell-long zigzag edge that a C_5 cluster is stably attached to the zigzag edge of $\theta_{G/Cu} = 0°$: C_5 attachment to the zigzag edge has an energy 0.29 eV lower than when adsorbed on the Cu substrate. Moreover, the attachment of an adatom to this configuration, $\theta_{G/Cu} = 0°$, is the most unstable (Figure 4b); thus we expect that the critical cluster size of stable attachment is C_5 or smaller, depending on $\theta_{G/Cu}$.

The key connection between this theoretically deduced mechanism of zigzag edge formation and our experimental findings of zigzag edges is the low carbon source concentration. The proposed mechanism occurs when sequential monomer attachment to the graphene edges occurs frequently, with cluster attachment occurring rarely. Clearly, this situation can be brought about by the use of a very low carbon feedstock concentration. Conversely, if the rate of growth by cluster attachment exceeds the rate of edge smoothing by monomer attachment, an irregular edge will be formed. Loginova *et al*. have shown that five-atom cluster attachment is the main process involved in CVD graphene growth on Ru(0001) surfaces[29] and that this leads to graphene edges that are not straight. These observations were modeled by Zangwill and Vvedensky,[30] whose analysis shows that inclusion of cluster and adatom attachment is required to explain all the experimental data, in accord with the growth mechanism proposed here.

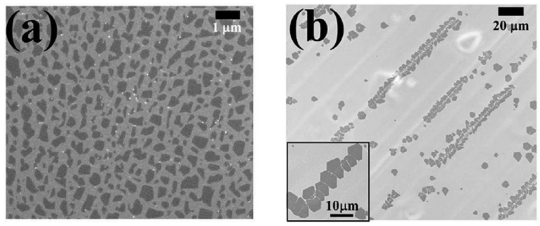

Figure 6. Altered growth conditions led to irregularly shaped graphene flakes. (a) Loss of symmetry due to high carbon source concentration (410 ppm). (b) Localized growth on micrometer-scale Cu grooves present on an unpolished copper substrate. Inset shows the loss of symmetry when edges between flakes are close.

The effect of carbon feedstock concentration is corroborated by our experimental results. As shown in Figure 6a, when a higher feedstock concentration of 410 ppm was used, the graphene seeds tended to lose their symmetry, and they took on a variety of shapes. The angles between neighboring edges were randomly distributed, with curved edges also frequently seen. Uniformity of the catalytic substrate also has an effect on graphene flake growth. As shown in Figure 6b, graphene flakes frequently grew preferentially on protruding parts of textured regions when as-provided (unpolished) substrates were used for the growth. On such samples, the graphene flakes were often packed along micrometer-scale grooves in the substrate. It was also observed that the regular hexagonal symmetry of the flakes was lost when they grew close to each other, possibly due to anisotropic carbon flux or spatially varying potential energy for adatoms within the very narrow channels between flakes. Our DFT calculations indicate that the adsorption energy of the carbon atoms on the Cu(100) surface is 0.74 eV higher than on the Cu(111) surface. This kind of orientation-dependent energy could lead to higher carbon concentration in grooves compared to flat regions of the substrate. An additional origin for the observed effects might be that rougher Cu surfaces are more reactive

than the Cu atoms in flat crystal planes, so that graphene seeds are more easily nucleated or pinned on such sites. The loss of hexagonal symmetry that accompanies increased carbon feedstock concentration or Cu roughness is consistent with our main experimental findings and proposed mechanism that low carbon flux leads to preferential monomer binding at armchair edges, promoting the growth of graphene flakes with pure zigzag edges.

CONCLUSIONS

In summary, we report a method of achieving control of the edge geometry of graphene crystallites and results of computational investigations that provide substantial insight into the growth mechanism. Atmospheric pressure CVD using polished catalytic Cu foil and low carbon feedstock concentration yields regular hexagonal graphene flakes as large as 100 μm on a side, with edges dominated by the zigzag direction, as evidenced by Raman spectroscopy and in agreement with an earlier report.[14] DFT calculations demonstrate that although zigzag and armchair edges have nearly equal formation energy on Cu, they differ strongly in the stability of single adsorbed carbon atoms, which should be a dominant consideration for growth at low feedstock concentration. Adatoms attached to zigzag edges and armchair−zigzag boundaries are energetically unstable. In contrast, monomer attachment to armchair edges is energetically favorable, which provides a mechanism of converting armchair edges to the zigzag geometry and maintaining the growth of straight zigzag edges. This work represents an important step forward in the understanding of the growth mechanisms for graphene by CVD and may provide a path toward the realization and even mass production of graphene nanodevices and atomically precise graphene electronics. In particular, we expect that highly crystalline zigzag edges would allow for precise control of spin state, which is critical for spintronics applications.

METHODS

Gases, including methane (purity 99.999% and 1% in argon), argon (99.999%), and hydrogen (99.999%) was purchased from GTS-Welco Inc. Cu foil (50 or 25 μm thick) was purchased from Alfa Aesar Inc. or McMaster-Carr Inc. Immediately before graphene growth, Cu foils were cleaned by sonicating in acetic acid for 5 min to remove the oxide layer. Solvents, including 100% ethanol, acetone, chemicals such as $FeCl_3 \cdot 6H_2O$ and HCl, and all other chemicals if not specified were purchased from Thermo Fisher Scientific Inc. All chemicals, if not specified, were used without further purification.

Procedures for electropolish of Cu foil, chemical vapor deposition growth of graphene films, and PMMA method for graphene film transfer are reported in previous publications.[15]

Raman Spectroscopy. Raman spectra of graphene samples on SiO_2/Si or PDMS substrates were obtained using a 514 nm excitation wavelength laser under a 100× objective. The laser power was kept below 4 mW to avoid damage to the sample.

Raman mapping measurements were preformed with an upright NTEGRA Spectra system (NT-MDT, Moscow, Russia), with lateral spatial resolution of ~400 nm. A green laser (λ = 532 nm) was used for excitation. All optical measurements were performed using a 100×/0.7 long working distance objective. A Peltier-cooled CCD detector (Andor Technologies, Ireland) with 1024 × 256 pixels was operated at −55 °C.

Supporting Information Available: Details of DFT calculations. This material is available free of charge *via* the Internet at http://pubs.acs.org.

Acknowledgment. Z.L., N.K., and A.T.C.J. were supported by the National Science Foundation through grant DMR-0805136 and the Nano/Bio Interface Center (NSF NSEC DMR0832802). S.K. was supported by the U.S. Department of Energy through grant DE-FG02-07ER15920, and A.M.R. by the Air Force Office of Scientific Research through FA9550-10-1-0248. Computational support was provided by the High-Performance Computing Modernization Office of the U.S. Department of Defense.

REFERENCES AND NOTES

1. Jia, X.; Hofmann, M.; Meunier, V.; Sumpter, B. G.; Campos-Delgado, J.; Romo-Herrera, J. M.; Son, H.; Hsieh, Y.-P.; Reina, A.; Kong, J.; Terrones; *et al*. Controlled Formation of Sharp Zigzag and Armchair Edges in Graphitic Nanoribbons. *Science* **2009**, *323*, 1701–1705.
2. Huang, B.; Liu, M.; Su, N.; Wu, J.; Duan, W.; Gu, B.-l.; Liu, F. Quantum Manifestations of Graphene Edge Stress and Edge Instability: A First-Principles Study. *Phys. Rev. Lett.* **2009**, *102*, 166404/1–166404/4.
3. Son, Y.-W.; Cohen, M. L.; Louie, S. G. Energy Gaps in Graphene Nanoribbons. *Phys. Rev. Lett.* **2006**, *97*, 216803.
4. Evaldsson, M.; Zozoulenko, I. V.; Heinzel, Xu, H.; Heinzel, T. Edge-Disorder-Induced Anderson Localization and Conduction Gap in Graphene Nanoribbons. *Phys. Rev. B* **2008**, *78*, 161407.
5. Barone, V.; Hod, O.; Scuseria, G. E. Electronic Structure and Stability of Semiconducting Graphene Nanoribbons. *Nano Lett.* **2006**, *6*, 2748–2754.
6. Son, Y.-W.; Cohen, M. L.; Louie, S. G. Half-Metallic Graphene Nanoribbons. *Nature* **2006**, *444*, 347–349.
7. Novoselov, K. S.; Geim, A. K.; Morozov, S. V.; Jiang, D.; Zhang, Y.; Dubonos, S. V.; Grigorieva, I. V.; Firsov, A. A. Electric Field Effect in Atomically Thin Carbon Films. *Science* **2004**, *306*, 666–669.
8. Casiraghi, C.; Hartschuh, A.; Qian, H.; Piscanec, S.; Georgi, C.; Fasoli, A.; Novoselov, K. S.; Basko, D. M.; Ferrari, A. C. Raman Spectroscopy of Graphene Edges. *Nano Lett.* **2009**, *9*, 1433–1441.
9. Krauss, B.; Nemes-Incze, P.; Skakalova, V.; Biro, L. P.; Klitzing, K. v.; Smet, J. H., Raman Scattering at Pure Graphene Zigzag Edges. *Nano Lett. 10*, 4544−4548.
10. Girit, C. O.; Meyer, J. C.; Erni, R.; Rossell, M. D.; Kisielowski, C.; Yang, L.; Park, C.-H.; Crommie, M. F.; Cohen, M. L.; Louie, S. G.; *et al*. Graphene at the Edge: Stability and Dynamics. *Science* **2009**, *323*, 1705–1708.
11. Datta, S. S.; Strachan, D. R.; Khamis, S. M.; Johnson, A. T. C. Crystallographic Etching of Few-Layer Graphene. *Nano Lett.* **2008**, *8*, 1912–1915.
12. Li, X.; Cai, W.; An, J.; Kim, S.; Nah, J.; Yang, D.; Piner, R.; Velamakanni, A.; Jung, I.; Tutuc, E.; *et al*. Large-Area Synthesis of High-Quality and Uniform Graphene Films on Copper Foils. *Science* **2009**, 1171245.
13. Bae, S.; Kim, H.; Lee, Y.; Xu, X.; Park, J.-S.; Zheng, Y.; Balakrishnan, J.; Lei, T.; Ri Kim, H.; Song, Y. I.; *et al*.

Roll-to-Roll Production of 30-in. Graphene Films for Transparent Electrodes. *Nat. Nanotechnol.* **2010**, *5*, 574–578.
14. Yu, Q.; Jauregui, L. A.; Wu, W.; Colby, R.; Tian, J.; Su, Z.; Cao, H.; Liu, Z.; Pandey, D.; Wei, D.; *et al*. Control and Characterization of Individual Grains and Grain Boundaries in Graphene Grown by Chemical Vapor Deposition. *Nat. Mater.* **2011**, *10*, 443–449.
15. Luo, Z.; Lu, Y.; Singer, D. W.; Berck, M. E.; Somers, L. A.; Goldsmith, B. R.; Johnson, A. T. C. Effect of Substrate Roughness and Feedstock Concentration on Growth of Wafer-Scale Graphene at Atmospheric Pressure. *Chem. Mater.* **2011**, *23*, 1441–1447.
16. Sutter, P. W.; Flege, J.-I.; Sutter, E. A. Epitaxial Graphene on Ruthenium. *Nat. Mater.* **2008**, *7*, 406–411.
17. McCarty, K. F.; Feibelman, P. J.; Loginova, E.; Bartelt, N. C. Kinetics and Thermodynamics of Carbon Segregation and Graphene Growth on Ru(0001). *Carbon* **2009**, *47*, 1806–1813.
18. N'Diaye, A. T.; Bleikamp, S.; Feibelman, P. J.; Michely, T. Two-Dimensional Ir Cluster Lattice on a Graphene Moiré on Ir(111). *Phys. Rev. Lett.* **2006**, *97*, 215501.
19. Li, X.; Cai, W.; Colombo, L.; Ruoff, R. S. Evolution of Graphene Growth on Ni and Cu by Carbon Isotope Labeling. *Nano Lett.* **2009**, *9*, 4268–4272.
20. Wofford, J. M.; Nie, S.; McCarty, K. F.; Bartelt, N. C.; Dubon, O. D. Graphene Islands on Cu Foils: The Interplay between Shape, Orientation, and Defects. *Nano Lett.* **2010**, *10*, 4890–4896.
21. You, Y.; Ni, Z.; Yu, T.; Shen, Z. Edge Chirality Determination of Graphene by Raman Spectroscopy. *Appl. Phys. Lett.* **2008**, *93*, 163112.
22. Ihm, J.; Zunger, A.; Cohen, M. L. Momentum-Space Formalism for the Total Energy of Solids. *J. Phys. C* **1979**, *12*, 4409–4422.
23. Rappe, A. M.; Rabe, K. M.; Kaxiras, E.; Joannopoulos, J. D. Optimized Psuedopotentials. *Phys. Rev. B* **1990**, *41*, 1227–1230.
24. Ramer, N. J.; Rappe, A. M. Designed Nonlocal Pseudopotentials for Enhanced Transferability. *Phys. Rev. B* **1999**, *59*, 12471.
25. Perdew, J. P.; Burke, K.; Ernzerhof, M. Generalized Gradient Approximation Made Simple. *Phys. Rev. Lett.* **1996**, *77*, 3865–3868.
26. Vanin, M.; Mortensen, J. J.; Kelkkanen, A. K.; Garcia-Lastra, J. M.; Thygesen, K. S.; Jacobsen, K. W., Graphene on Metals: A van der Waals Density Functional Study. *Phys. Rev. B 81*, 081408.
27. Barrett, C. S.; Massalski, T. B. *Structure of Metals: Crystallographic Methods, Principles and Data*; Barrett, C. S., Massalski, T. B., Eds.; Pergamon: Oxford, 1980.
28. Koskinen, P.; Malola, S.; Häkkinen, H. Evidence for Graphene Edges beyond Zigzag and Armchair. *Phys. Rev. B* **2009**, *80*, 073401.
29. Loginova, E.; Bartelt, N. C.; Feibelman, P. J.; McCarty, K. F. Evidence for Graphene Growth by C Cluster Attachment. *New J. Phys.* **2008**, *10*, 093026.
30. Zangwill, A.; Vvedensky, D. D. Novel Growth Mechanism of Epitaxial Graphene on Metals. *Nano Lett.* **2011**, *11*, 2092–2095.